



Published in final edited form as:

Clin Cancer Res. 2009 March 1; 15(5): 1747–1754. doi:10.1158/1078-0432.CCR-08-1420.

DCE-MRI as a Biomarker for Prediction of Radiation-Induced Neurocognitive Dysfunction

Y. Cao^{1,2}, C.I. Tsien¹, P.C. Sundgren², V. Nagesh¹, D. Normolle¹, H. Buchtel^{3,5}, L. Junck⁴, and T.S. Lawrence¹

¹Department of Radiation Oncology, University of Michigan, Ann Arbor, MI

²Department of Radiology, University of Michigan, Ann Arbor, MI

³Department of Psychiatry, University of Michigan, Ann Arbor, MI

⁴Department of Neurology University of Michigan, Ann Arbor, MI

⁵VA Ann Arbor Healthcare System

Abstract

Purpose—To determine whether early assessment of cerebral microvessel injury can predict late neurocognitive dysfunction after brain radiation therapy (RT).

Experimental Design—Ten patients who underwent partial brain RT participated in a prospective dynamic contrast-enhanced (DCE) MRI study. DCE-MRI was acquired prior to, at week 3 and 6 during, and 1 month and 6 months after RT. Neuropsychological tests were performed pre-RT and at the post-RT MRI follow-ups. The correlations between early delayed changes in neurocognitive functions and early changes in vascular parameters during RT were analyzed.

Results—No patients had tumor progression up to 6 months after RT. Vascular volumes and blood-brain barrier (BBB) permeability increased significantly in the high dose regions during RT by 11% and 52% ($P < .05$), respectively, followed by a decrease after RT. Changes in both vascular volume and BBB permeability correlated with the doses accumulated at the time of scans at week 3 and 6 during RT and 1 month after RT ($P < .03$). Changes in verbal learning scores 6 months after RT were significantly correlated with changes in vascular volumes of left temporal ($p < .02$) and frontal lobes ($P < .03$) and changes in BBB permeability of left frontal lobes during RT ($P < .007$). Similar correlation was found between recall scores and BBB permeability.

Conclusion—Our data suggest that the early changes in cerebral vasculature may predict delayed alterations in verbal learning and total recall, which are important components of neurocognitive function. Additional studies are required for validation of these findings.

Corresponding author: Yue Cao, Ph.D. UH-B2C432, Box 0010 Departments of Radiation Oncology and Radiology University of Michigan Ann Arbor, MI 48109–0010 Phone: (734)647–2914 Fax: (734)936–7859 Email: yuecao@umich.edu.

Statement of Clinical Relevance

Neurotoxicity is a major clinical complication following radiation therapy of brain tumors. Clinical symptoms can occur acutely and subacutely, but most devastating neurotoxicity manifests with late neurological sequelae, including neurocognitive dysfunction, white matter degeneration, and necrosis. Late neurocognitive dysfunction presents as diminishing mental capacity for working memory, learning ability, executive function, and attention. Recent multi-center studies of patients with low-grade gliomas who are without clinical signs of tumor recurrence after radiation treatment show that both high total dose as well as high dose per fraction are associated with neurocognitive deterioration, especially related to memory functions. Given the delayed nature of neurocognitive dysfunction, it would be valuable to identify biomarkers, including those derived from in vivo imaging, for early assessment of individual sensitivity to radiation and prediction of late neurotoxicity. Such biomarkers might provide an opportunity to individualize the dose of radiation therapy or to begin neuroprotective therapy. This study aims to address this clinically relevant question.

Keywords

Normal tissue toxicity; blood volume; DCE MRI; dose volume effect

Radiation therapy (RT) is a major treatment modality for malignant and benign brain tumors. The major limiting factor in its use is neurotoxicity. This neurotoxicity manifests as late neurological sequelae and neurocognitive dysfunctions with or without gross tissue necrosis (1-4). Late neurocognitive dysfunction prominently affects working memory, learning ability, executive function, and attention span. Although a few studies find that tumor progression is associated with deterioration of neurocognitive function after RT (5-7), a recent multi-center study of patients with low-grade gliomas who had no clinical signs of tumor recurrence at least one year after partial brain (90% of the patients) or whole brain RT showed that a high total dose correlated with a decline in working memory and that a high dose per fraction interferes with long-term memory storage and retrieval (4). Also, in a randomized trial of low- (50.4 Gy) versus high-dose (64.8 Gy) partial brain RT in patients with supratentorial low-grade glioma, significant cognitive deteriorations from baseline were found in those without tumor progression, with rates of 8.2%, 4.6%, and 5.3% at years of 1, 2, and 5 respectively, as assessed by the Folstein Mini-Mental State Examination (MMSE) (8), a relatively crude measure of neurocognitive function. Moreover, the rate of cognitive impairment in patients undergoing partial brain RT is even higher when assessed using a battery of neuropsychological tests that are much more sensitive to cognitive functions than the MMSE (4,9-12). The potential effect of RT on neurocognitive outcomes is an important factor in the determination of the risks versus benefits of treatment (13), which should be an integral part of clinical decision-making. Given the delayed nature of neurocognitive dysfunction, it would be important to identify biomarkers for early assessment and prediction of late neurotoxicity.

Radiation-induced injury in cerebral tissue is a highly complex and interactive process involving multiple tissue elements (2,14,15). Vascular injury has long been considered to be of crucial importance for the development of cerebral tissue toxicity in response to irradiation. A large body of evidence suggests that vascular injury occurs acutely and precedes subacute demyelination and reactive astrocytic and microglial responses (16-19). Early histopathologic changes in blood vessels after irradiation include dilation and thickening of blood vessels, endothelial cell nuclear enlargement, and hypertrophy of perivascular astrocytes. The dose-dependent endothelial cell death and apoptosis occur as early as 24 hours after irradiation (17,18). The initial injury of vessels is followed by the formation of platelet matrix and thrombi, which eventually results in occlusion and thrombosis in microvessels within weeks to months (14,20,21). Furthermore, cerebral vascular injury is followed by degenerative structural changes in white matter (22-25). The time lag between vascular injury and demyelination and necrosis in white matter diminishes with increased dose (22). Most of these histopathologic and biologic studies have been carried out in rodent models using a single large dose of radiation. Whether the dose- and time-dependent changes in histopathology in the human brain after 5–6 weeks fractionated RT have the same biological sequences has yet to be determined. However, the more serious effects causing neurological symptoms, including gross white matter necrosis and degeneration, are late effects that generally do not occur until 12 months or more after the completion of RT (1,2).

Few prospective studies have investigated the effects of radiation on the human brain during a course of radiation and then after treatment over time. One of our previous studies assessed the temporal changes in normal-appearing large white matter fibers longitudinally, and revealed progressive changes beginning early in the course of RT to nine months after the completion of RT (26). If there are early changes in cerebral vasculature, as has been observed in animal models, and if the early changes in vasculature are associated with late white matter

degeneration and/or late neurological symptoms and neurocognitive dysfunction, then early vascular changes could be a biomarker for late neurotoxicity.

We conducted a prospective study to investigate three questions: (a) how cerebral blood vessels in normal tissue of patients who undergo partial brain RT change over time: (b) how these changes are related to dose and dose-volume: and (c) if these changes are associated with neurocognitive dysfunction. We hypothesized that early monitoring of cerebral blood microvessels in response to fractionated RT would allow prediction of late neurocognitive deficits. This predictive ability would permit identification of a time window for neuroprotective therapeutic intervention.

MATERIAL AND METHODS

Patients

Ten patients with newly diagnosed low-grade glioma, meningioma, cranopharyngioma or benign tumor underwent three-dimensional conformal cranial RT with a median dose of 54 Gy (range: 50.4–59.4 Gy in 1.8 Gy fractions), and participated in a prospective, Institutional Review Board approved, clinical magnetic resonance imaging (MRI) study (Table 1). The overall degree of physical function was assessed by using the Karnofsky Performance Status Scale, which was ≥ 90 prior to RT in all but one patient (who had a Karnofsky of 80), indicating these patients were highly functioning.

DCE-MRI

Patients underwent an MRI 1–2 weeks prior to RT, at weeks 2–3 and weeks 5–6 during the course of RT, and at 1 month and 6 months following the completion of RT. All MRI scans were performed on a 1.5-Tesla scanner (General Electric Health Care, WI). MRI series included T1-weighted images, T2-weighted fluid-attenuated inversion recovery (FLAIR) images, diffusion tensor images, dynamic contrast-enhanced (DCE) T1-weighted images, post-contrast T1-weighted images, and two-dimensional proton spectroscopy images. DCE images were acquired with a 3D gradient echo pulse sequence with TE/TR = 1.08/3.4 ms, flip angle = 20°, field-of-view = 220 × 220 × 132 mm³, matrix size = 256 × 256 × 22, spatial resolution = 0.86 × 0.86 × 6 mm³, and temporal resolution = 7.2s. The 3D slab was acquired in the sagittal plane to eliminate the time-of-flight effect from in-flow blood proton spins. A total of 38 dynamic volumes were acquired during 274 s. A single dose (0.1 mL/kg) of Gd-DTPA was injected at 2 ml/sec, during which DCE image volumes were acquired. In this study, we focused on the analysis of DCE images and changes of parameters estimated from the DCE data over time.

Image Registration

All images including anatomic MRI, DCE-MRI, and treatment planning CT were co-registered by using the Mutual Information and Simplex optimization algorithm implemented in an in-house Functional Image Analysis Tool (FIAT).⁽²⁷⁾ DCE images were first registered within the series to correct possible mis-alignment prior to estimations of kinetic parameters (described in detail below). After estimating kinetic parameters, all sagittal parametric maps obtained at different follow-up times were co-registered to the axial post-contrast T1-weighted images acquired prior to RT. Finally, through co-registration of treatment planning CT with MRI, the planned dose distribution map was also co-registered with MRI.

Estimation of Kinetic Parameters from DCE-MRI

The modified Toft model was used to estimate kinetic parameters (28). In this model, the parameters considered include the transfer constant (K^{trans}) for gadolinium (Gd) influx from the intravascular space into the extravascular extracellular space, the fractional plasma volume

(V_p) in tissue, and the back-flux constant rate for gadolinium efflux from the extravascular extracellular space back to the intravascular space. A small vessel hematocrit value of 0.45 was used. The artery input function was obtained from carotid arteries by thresholding to determine the earliest contrast uptake. Note that the V_p obtained by this model was corrected for vascular leakage.

Temporal Change and Dose Effect

We focused on the temporal change of the fractional volume of blood plasma (V_p) and the transfer constant (K^{trans}) of Gd-DTPA from intravascular space into the extravascular extracellular space in normal-appearing cerebral tissue, which is defined as the cerebral tissue that appears normal on T1-weighted images and FLAIR images from pre RT to 6 months after the completion of RT. Changes in K^{trans} reflect changes in blood-brain-barrier (BBB) permeability to Gd-DTPA. To assess the changes in V_p and K^{trans} in relation to the radiation dose, cerebral tissue was divided into seven intervals based upon receiving a biologically-equivalent dose of 2 Gy per fraction (bio-dose, $\alpha/\beta = 2.5$), as 0–5 Gy, 5–10 Gy, 10–20 Gy, 20–30 Gy, 30–40 Gy, 40–50 Gy, and > 50 Gy. The means of the bio-dose in the seven volumes of interest and the means of V_p were calculated. To assess the effect of dose-volume, the brain volumes that received 0–20 Gy, 20–40 Gy, and > 40 Gy were computed based upon the treatment planning CT and dose distribution.

Neurocognitive Function Tests

All patients underwent a battery of standardized neurocognitive tests prior to RT and at each of the post-RT MRI follow-ups. The neurocognitive tests included Trail Making Tests A and B (29), the Hopkins Verbal Learning Test (HVLT) (30,31), and the Controlled-Oral Word Association (COWA) (32,33). Trail Making Test A assesses information processing efficiency. Trail Making Test B and COWA assess executive function. HVLT assesses verbal memory (recall, delayed recall, and recognition components) and learning (learning component). In addition, the MMSE was administered. These neuropsychological tests were used in RTOG trials of prophylactic cranial irradiation for patients with limited small cell lung cancer disease (RTOG 0212) and motexafin gadolinium and whole-brain radiation for patients with brain metastases (5). All tests were administered by trained and certified research associates for RTOG trials and standards.

A score of 1.5 standard deviations (SD) below the mean of age-matched normative data has been considered to have impairment in neurocognitive function (30,31). Therefore, if a score of a neurocognitive test in a patient prior to RT was 1.5 SD below the mean of the age-matched normative data, the patient was considered to have pre-existing neurocognitive function impairment.

Statistical Methods

The linear mixed model was used to assess the dose effect and the dose-volume effect on the brain vasculature properties of V_p and K^{trans} . First, we tested the dose effect at the different time points, during the course of RT and after the completion of RT, to evaluate the evolution of the dose effect over time. The linear mixed model was considered as:

$$\Delta P_{ijt} = \alpha_t + \beta_t \times D_{ijt} + a_{it}, \quad [1]$$

where subscripts i , j , and t denote respective subject, region, and time, ΔP is the change of V_p or K^{trans} observed at time t compared to that patient's baseline, and D_{ijt} is the biologically-corrected dose received in region j of subject i by time t . β_t is the slope at time t , and its change over time would suggest the dose effect evolving. α_t and a_{it} are the global intercept and the

individual subject intercept at time t , respectively. Second, we tested the dose-volume effect as a possible additional factor contributed to injury of the cerebral vasculature. The model was tested given by:

$$\Delta P_{ijt} = \alpha_t + \beta_t \times (D_{ijt} \times V_{ik}) + a_{it}, \quad [2]$$

where V_{ik} is the dose-volume of either V_{0-20} , V_{20-40} or $V_{>40}$ for patient i . Given that the three dose volumes are correlated, only one dose volume can be added into the model each time.

The correlations between the early changes in V_p and K^{trans} during the course of RT and the early delayed changes (6 months after RT) in neurocognitive functions were tested by Pearson correlation coefficient. Because we predicted the direction of expected changes, one tailed P-values of <0.05 were considered to be significant.

RESULTS

Clinical and Radiological Findings

None of the patients evidenced tumor progression at 6 months (of 10 eligible patients) or 18 months (of 5 eligible patients) after the completion of RT. Also, none of the ten patients showed gross radiation-induced lesions on T2-weighted FLAIR and post-Gd T1-weighted images up to 6 months after radiation therapy. All patients with glioma and the patient with ependymoma had associated signal increases on T2-weighted FLAIR images in the tumor and in its vicinity prior to RT. These tumor-related hyperintensities on T2-weighted FLAIR images did not substantially change during the 6 month follow-up. In one patient with glioma, mild scattered focal areas of increased T2/FLAIR signal abnormalities were present in the centrum semiovale and periventricular white matter prior to RT, consistent with old ischemic changes. These areas demonstrated no further change over time. No additional areas of radiation-induced abnormalities were present during follow-up. In patients with pituitary adenomas and in the patient with craniopharyngioma, no signal abnormality outside the tumor was present pre treatment and no interval change was seen during the 6 month follow-up. In the patient with sphenoid wing meningioma, post-surgical changes were demonstrated, and no changes on T2 and FLAIR signals beyond the surgical cavity were seen over the six month follow-up.

Temporal Changes in Vascular Volumes and BBB Permeability

The averaged fractional volume of blood plasma (V_p) (representing the vascular volume when corrected with hematocrit) in normal-appearing cerebral tissue in the patients was 1.4 mL/100 g prior to RT, which is in the normal range. The temporal changes in V_p exhibited a complex pattern in relation to radiation dose parameters. First, the temporal changes in V_p were evaluated in three dose intervals as 0–20 Gy, 20–40 Gy, and > 40Gy, which have been used in previous studies to assess the dose-volume effect (34). The time courses of the changes in V_p depended on the dose received by the tissue regions (Figure 1). For the cerebral tissue regions that received the low dose (0–20 Gy), V_p exhibited non-significant changes ($P > .05$). In the tissue regions that received 20–40 Gy, V_p increased by 4% (0.05 ± 0.08 mL/100 g, mean \pm SE) at week 3 during RT. The increase reached 7% (0.10 ± 0.05 mL/100g) at week 6 during RT and by 12% (0.16 ± 0.10 mL/100g) 1 month after the completion of RT. The increase was significant at week 6 during RT ($p=.05$). Then, at 6 months after the completion of RT, V_p decreased from the value observed 1 month after RT and returned to the value of week 3 during RT (Figure 1), suggesting that in this intermediate dose range vessels are dilated initially and then either return to normal or undergo regression. In the brain region that received > 40 Gy, V_p rapidly increased by 10% (0.14 ± 0.09 mL/100 g) at week 3 during the course of RT, and by 11% (0.15 ± 0.07 mL/100g) at week 6 during RT, approximately the maximum value observed in the 20

–40 Gy brain region 1 month after RT. The increase in V_p at week 6 during of RT was significant ($P < .05$). After the completion of RT, V_p values decreased from the elevated values during RT to a value at 6 months (0.10 ± 0.10 mL/100 g) that was still 7% greater than the baseline value, suggesting that this higher dose range evokes rapid vessel dilation, followed by vessel regression or renormalization after the completion of RT. The transition occurred sooner in the high dose range than the intermediate dose range.

Temporal profiles of the changes in K^{trans} (reflecting BBB permeability to Gd-DTPA) of normal-appearing brain were similar to those in V_p (Figure 1). In the regions received low doses (0–20 Gy), K^{trans} exhibited non-significant changes. In the region received 20–40 Gy, K^{trans} values increased significantly by 39% ($0.042 \pm 0.016 \times 10^{-2} \times \text{min}^{-1}$) at week 6 during the course of RT ($P < .02$). After the completion of RT the K^{trans} values started to decrease from the elevated values at the end of RT, but still remained elevated by 23% ($0.025 \pm 0.014 \times 10^{-2} \times \text{min}^{-1}$) 1 month post RT, and eventually returned to the pre-RT values 6 months post RT. In the tissue region received >40Gy, the K^{trans} values were increased significantly by 52% ($0.057 \pm 0.019 \times 10^{-2} \times \text{min}^{-1}$) at week 6 during the course of RT ($P < .01$). After the completion of RT the K^{trans} values decreased from the elevated values at the end of RT, which is similar to the temporal pattern that we observed previously in the tumor of a different group of the patients (35).

Dose Effects

The dose effects on the cerebral vasculature were analyzed using the linear mixed model. In model 1 (Eq. [1]), only the dose effect on the cerebral vasculature and the evolution of the dose-dependency changes over time were examined. The dose-dependence of V_p was the largest at week 3 during the course of RT ($P < .0001$, Table 2). At week 6 of RT, the dose-dependence of V_p was high ($P < .0001$), but even though the dose received by tissue was approximately double that at week 3, the dose-dependence of V_p was approximately half of the one observed at week 3 (Table 2). After the completion of RT, the dose-dependent change in V_p continued decreasing, and by 6 months after RT, the dose-dependence of V_p was diminished. This evolution of the dose-dependent changes in V_p can also be seen in the scatter plots of Figure 2.

Using the linear mixed model, the changes in K^{trans} (BBB permeability to Gd-DTPA) both during the course of RT and after the completion of RT were found to depend significantly upon the accumulated doses at the time of the MRI observation (P values from 0.001 to 0.03, Table 2 and Figure 2). The linear slopes (β_t) that reflect K^{trans} value changes per unit dose were 2.0×10^{-5} , 7.8×10^{-6} , 6.1×10^{-6} , and $4.5 \times 10^{-6} \text{ min}^{-1}$ per Gy at week 3 and week 6 during the course of RT and 1 month and 6 months after the completion of RT, respectively, indicating the strongest dose-response at week 3 during RT.

Dose-Volume Effects

To evaluate whether the volume of brain irradiated affects blood volume in addition to the dose, we developed model 2 which includes the dose-volume effect (Eq. [2]). The changes in V_p were found to depend on the product of the bio-dose received at the time of observation and the volume of brain receiving a total dose > 40 Gy ($V_{>40}$), indicating that the effect of higher doses of radiation was greater with increasing brain volume irradiated with the high doses (Table 2). The dose and dose-volume ($D * V_{>40}$) dependent changes in V_p were significant both during and after the completion of RT (Table 2). Again, the strongest interactive effect of the dose and the dose-volume on V_p was observed at week 3 during the course of RT, and the effect remained significant 6 months after the completion of treatment ($P < .007$, Table 2).

There was no significant dose-volume effect on K^{trans} values found by the linear mixed model.

Neurocognitive Function Changes

All patients had MMSE scores of 27 or above prior to RT, and this measure showed little change over the 6 months after the completion of RT (Table 3). HVLt assesses multiple verbal memory and learning components, e.g., recall, learning and delayed recall. Scores of total recall (sum of three trials), learning, and delayed recall (20 minutes delay) pre RT, and 1 month and 6 months after the completion of RT are given in Table 3. Prior to RT, the total recall scores of five patients were more than 1.5 SDs below the means of the age-matched normative data; the delayed recall scores of three patients were more than 1.5 SDs below the means of their age-matched normative data, indicating pre-RT existing conditions in several of the patients. Three patients had borderline impaired learning scores, approximately 1.5 SD below the means of the age-matched normative data, indicating that pre-RT memory abilities were more compromised than learning abilities in these patients in terms of both severity and frequency.

Next, we tested the association between early changes in V_p and K^{trans} during the course of RT and early delayed changes (6 months after the completion of RT) in HVLt recall, learning, and delayed recall scores. We found that the changes in the verbal learning scores 6 months after RT compared to pre RT were correlated significantly with the percentage changes in V_p of left frontal lobes ($P = .032$) and left temporal lobes ($P = .017$) at week 3 during the course of RT (Figure 3). There was no significant correlation between the early delayed changes in learning scores and the early changes in V_p of right frontal or temporal lobes, consistent with presumed left hemisphere predominance for language and therefore for verbal learning. The declines in verbal learning scores 6 months after RT vs pre-RT were significantly correlated with the percentage changes in K^{trans} of left frontal lobes at week 3 during the course of RT ($P = .007$), and but not with the changes in K^{trans} of right frontal lobes or left and right temporal lobes at week 3 during RT. There was no significant correlation between the early delayed changes in total recall or delayed recall scores and the early changes in V_p during the course of RT of left or right frontal or temporal lobes. The changes in total recall scores 6 months after RT were significantly correlated with the percentage changes in K^{trans} of left temporal lobes ($P = 0.028$) at week 3 during the course of RT. There was no significant correlation between the early delayed changes in Trail Making B or COWA and the early changes in V_p or K^{trans} during the course of RT of left or right frontal or temporal lobes.

DISCUSSION

In this study, we assessed the early vascular changes during the course of RT and the changes that occurred up to 6 months after the completion of RT. The vascular volume and BBB permeability demonstrated an initial increase during the course of RT, and then a gradual decrease after the completion of RT. The regions receiving the highest doses showed the most rapid and significant changes. The initial increase in the vascular volume is most likely due to vessel dilation in response to accumulated modest amounts of doses (14,15,17,22,23). The early delayed decrease represents either vascular regression such as capillary collapse and occlusion after progressive loss of endothelial cells and formation of platelet clusters and thrombi (14,17,18,21) or vessel renormalization. The temporal profile of the changes in BBB permeability of normal tissue is similar to what we have observed previously in the tumor of a different patient population (35). The increase in BBB permeability could be due to endothelial cell death and apoptosis in response to irradiation, which is directly correlated to the dose. However, the dose-effect on the cerebral vasculature volume is observed during the course of RT, and then diminishes over time after the completion of RT; while the dose-volume effect persists up to 6 months after RT. This evolution from the dose-effect to the dose-volume effect previously has not been demonstrated. Finally, these early changes (week 3 during the course of RT) in the cerebral vascular volume and BBB permeability are associated with the early delayed changes in learning and recall scores of HVLt. These findings suggest that the

early changes in the cerebral vasculature may predict delayed changes in verbal learning and total recall, which are key components in neurocognitive function. Additional studies are required for validation of these findings.

Our understanding of the histopathologic and biologic changes in cerebral vasculature and tissue after RT is derived mainly from the studies of rodent models. Most of these studies have been carried out by using a single dose of modest to high size, although some recent studies have used fractionated radiation (21,36). One such study that used 2 Gy per fraction for a total of 40 Gy over 4 weeks in mice found no early blood-brain barrier disruption until 90 days after the completion of fractionated irradiation (36). In the present study, we found early vascular changes including the vessel volume and blood-brain barrier disruption, in which the most apparent changes were seen in the brain regions that receive > 40 Gy. Nevertheless, several studies of rodent models report early vascular changes after a single dose;(17,18) the time course of the progressive injury of cerebral tissue in these models differs somewhat from what we observe in humans who receive fractionated RT (2,14,15,22). In clinical studies, T2 lesions are located predominantly in periventricular regions, indicating demyelination, and start appearing 2–6 months after RT. The T2 lesions increase over the next year. Necrosis does not occur until a year after RT. In the rodent models, a commonly observed pattern of cerebral tissue injury begins with early vascular injury as vessel dilation and endothelial apoptosis and cell death, progresses to subacute demyelination, and is followed by vessel thrombi and diminution, diffuse demyelination, and necrosis. The major discrepancy between clinical observations and rodent models seems to be a lack of the equivalence of the doses to produce similar symptoms. Given that it is extremely difficult to obtain human brain samples to study cerebral normal tissue injury after RT, we must continue to rely on animal models including rodents to understand the histopathology and biology of radiation-induced neurotoxicity. However, extrapolating findings from animal models to humans needs to be done with caution.

The radiation dosimetry parameters, such as total dose, fraction size, and dose-volume distribution, affect late brain tissue degeneration and neurological and neurocognitive sequelae in a complex fashion. Our knowledge of the dose-volume effect on the human brain is derived primarily from the reports of late neurological sequelae and neurocognitive dysfunctions of long-term survivors who have undergone whole brain radiation (3,9). However, the effect of dose-volume distribution on cerebral tissue injury and neurocognitive outcomes is less clear for partial brain irradiation. Recent efforts have been to develop statistical models to determine the dose-volume distribution in relation to children's IQ scores months and years after cranial irradiation treatment (34). In the present study, we found that high dose had a greater effect in the patient in whom a large volume of the brain received the high dose. Our preliminary findings indicate that reducing the volume of the brain that receives high doses, e.g. by intensity modulated radiation therapy, may benefit the patients who have a reasonable prospect for long-term survival.

It has been recognized in recent years that the radiation doses below the threshold of causing tissue necrosis pose risks for patients' cognitive functions years after cranial irradiation (4,8). For instance, the vascular changes after partial rodent brain irradiation by doses both above and below the threshold of necrosis are associated with impairments of cognitive functions, while the low dose impacts cognitive functions to a lesser extent (37). In the present study, we demonstrate the association between early vascular changes and early delayed neurocognitive function changes in the patients who received 50.4–59.4 Gy with 1.8 Gy/fraction, in whom no radiation-induced necrosis or white matter abnormality were observed on conventional MRI up to 6 months after RT. Patient variations in tumor locations most likely contribute to neurocognitive abnormalities prior to RT and possibly after RT. In our patients, the verbal learning scores of HVLT prior to RT ranged from borderline deficient to normal and were less compromised by the pre-RT conditions than total recall and delayed recall. There were

consistent correlations between the early delayed changes in learning scores and the early changes in the two vascular parameters. It is important to point out that the changes in learning, total recall, and delayed recall scores 6 months after RT were not correlated with the dose, the dose-volume or the interaction of the dose and dose-volume in either left or right frontal or temporal lobes ($P > 0.5$, data are not showed), suggesting that dosimetric parameters may not be good surrogates for late delayed neurocognitive function outcomes. This is primarily due to individual sensitivity to radiation, which is not accounted for in the dosimetric parameters. A better prediction for the delayed clinical symptoms and neurocognitive outcomes may be gained from assessing individual patient responses to radiation. In one of our recent works, we have demonstrated that substantial differences exist between individual patients in the sensitivity of the liver to radiation (38). Assessing individual risks for brain injury after irradiation using functional imaging could allow us to develop individualized patient treatment strategies, which would likely improve outcomes and patient quality of life.

Acknowledgments

This work is supported in part by 3 PO1 CA59827 and R21 CA113699. The authors would like to thank Kristin Brierley for coordinating the study, Diana Li for data management, and Zhou Shen for programming support.

REFERENCES

- Schultheiss TE, Kun LE, Ang KK, Stephens LC. Radiation response of the central nervous system. *Int J Radiat Oncol Biol Phys* 1995;31(5):1093–112. [PubMed: 7677836]
- Tofilon PJ, Fike JR. The radioresponse of the central nervous system: a dynamic process. *Radiat Res* 2000;153(4):357–70. [PubMed: 10798963]
- Khuntia D, Brown P, Li J, Mehta MP. Whole-brain radiotherapy in the management of brain metastasis. *J Clin Oncol* 2006;24(8):1295–304. [PubMed: 16525185]
- Klein M, Heimans JJ, Aaronson NK, van der Ploeg HM, Grit J, Muller M, Postma TJ, Mooij JJ, Boerman RH, Beute GN, Ossenkoppele GJ, van Imhoff GW, Dekker AW, Jolles J, Slotman BJ, Struikmans H, Taphoorn MJ. Effect of radiotherapy and other treatment-related factors on mid-term to long-term cognitive sequelae in low-grade gliomas: a comparative study. *Lancet* 2002;360(9343):1361–8. [PubMed: 12423981]
- Mehta MP, Shapiro WR, Glantz MJ, Patchell RA, Weitzner MA, Meyers CA, Schultz CJ, Roa WH, Leibenhaut M, Ford J, Curran W, Phan S, Smith JA, Miller RA, Renschler MF. Lead-in phase to randomized trial of motexafin gadolinium and whole-brain radiation for patients with brain metastases: centralized assessment of magnetic resonance imaging, neurocognitive, and neurologic end points. *J Clin Oncol* 2002;20(16):3445–53. [PubMed: 12177105]
- Meyers CA, Brown PD. Role and relevance of neurocognitive assessment in clinical trials of patients with CNS tumors. *J Clin Oncol* 2006;24(8):1305–9. [PubMed: 16525186]
- Armstrong CL, Goldstein B, Shera D, Ledakis GE, Tallent EM. The predictive value of longitudinal neuropsychologic assessment in the early detection of brain tumor recurrence. *Cancer* 2003;97(3):649–56. [PubMed: 12548607]
- Brown PD, Buckner JC, O'Fallon JR, Iturria NL, Brown CA, O'Neill BP, Scheithauer BW, Dinapoli RP, Arusell RM, Curran WJ, Abrams R, Shaw EG. Effects of radiotherapy on cognitive function in patients with low-grade glioma measured by the folstein mini-mental state examination. *J Clin Oncol* 2003;21(13):2519–24. [PubMed: 12829670]
- Roman DD, Sperduto PW. Neuropsychological effects of cranial radiation: current knowledge and future directions. *Int J Radiat Oncol Biol Phys* 1995;31(4):983–98. [PubMed: 7860415]
- Postma TJ, Klein M, Verstappen CC, Bromberg JE, Swennen M, Langendijk JA, Taphoorn MJ, Scheltens P, Slotman BJ, van der Ploeg HM, Aaronson NK, Heimans JJ. Radiotherapy-induced cerebral abnormalities in patients with low-grade glioma. *Neurology* 2002;59(1):121–3. [PubMed: 12105319]

11. Crossen JR, Garwood D, Glatstein E, Neuwelt EA. Neurobehavioral sequelae of cranial irradiation in adults: a review of radiation-induced encephalopathy. *J Clin Oncol* 1994;12(3):627–42. [PubMed: 8120563]
12. Armstrong CL, Hunter JV, Ledakis GE, Cohen B, Tallent EM, Goldstein BH, Tochner Z, Lustig R, Judy KD, Pruitt A, Mollman JE, Stanczak EM, Jo MY, Than TL, Phillips P. Late cognitive and radiographic changes related to radiotherapy: initial prospective findings. *Neurology* 2002;59(1):40–48. [PubMed: 12105305]
13. Mulhern RK, Palmer SL, Merchant TE, Wallace D, Kocak M, Brouwers P, Krull K, Chintagumpala M, Stargatt R, Ashley DM, Tyc VL, Kun L, Boyett J, Gajjar A. Neurocognitive consequences of risk-adapted therapy for childhood medulloblastoma. *J Clin Oncol* 2005;23(24):5511–9. [PubMed: 16110011]
14. Belka C, Budach W, Kortmann RD, Bamberg M. Radiation induced CNS toxicity--molecular and cellular mechanisms. *Br J Cancer* 2001;85(9):1233–9. [PubMed: 11720454]
15. Wong CS, Van der Kogel AJ. Mechanisms of radiation injury to the central nervous system: implications for neuroprotection. *Mol Interv* 2004;4(5):273–84. [PubMed: 15471910]
16. Price RE, Langford LA, Jackson EF, Stephens LC, Tinkey PT, Ang KK. Radiation-induced morphologic changes in the rhesus monkey (*Macaca mulatta*) brain. *J Med Primatol* 2001;30(2):81–7. [PubMed: 11491408]
17. Ljubimova NV, Levitman MK, Plotnikova ED, Eidus L. Endothelial cell population dynamics in rat brain after local irradiation. *Br J Radiol* 1991;64(766):934–40. [PubMed: 1954536]
18. Pena LA, Fuks Z, Kolesnick RN. Radiation-induced apoptosis of endothelial cells in the murine central nervous system: protection by fibroblast growth factor and sphingomyelinase deficiency. *Cancer Res* 2000;60(2):321–7. [PubMed: 10667583]
19. Li YQ, Chen P, Haimovitz-Friedman A, Reilly RM, Wong CS. Endothelial apoptosis initiates acute blood-brain barrier disruption after ionizing radiation. *Cancer Res* 2003;63(18):5950–6. [PubMed: 14522921]
20. Verheij M, Dewit LG, Boomgaard MN, Brinkman HJ, van Mourik JA. Ionizing radiation enhances platelet adhesion to the extracellular matrix of human endothelial cells by an increase in the release of von Willebrand factor. *Radiat Res* 1994;137(2):202–7. [PubMed: 8134544]
21. Brown WR, Thore CR, Moody DM, Robbins ME, Wheeler KT. Vascular damage after fractionated whole-brain irradiation in rats. *Radiat Res* 2005;164(5):662–8. [PubMed: 16238444]
22. Reinhold HS, Calvo W, Hopewell JW, van der Berg AP. Development of blood vessel-related radiation damage in the fimbria of the central nervous system. *Int J Radiat Oncol Biol Phys* 1990;18(1):37–42. [PubMed: 2298633]
23. Calvo W, Hopewell JW, Reinhold HS, Yeung TK. Time- and dose-related changes in the white matter of the rat brain after single doses of X rays. *Br J Radiol* 1988;61(731):1043–52. [PubMed: 3208008]
24. Okeda R, Okada S, Kawano A, Matsushita S, Kuroiwa T. Neuropathology of delayed encephalopathy in cats induced by heavy-ion irradiation. *J Radiat Res (Tokyo)* 2003;44(4):345–52. [PubMed: 15031561]
25. Fike JR, Sheline GE, Cann CE, Davis RL. Radiation necrosis. *Prog Exp Tumor Res* 1984;28:136–51. [PubMed: 6484197]
26. Nagesh V, Tsien CI, Chenevert TL, Ross BD, Lawrence TS, Junick L, Cao Y. Radiation-induced changes in normal-appearing white matter in patients with cerebral tumors: a diffusion tensor imaging study. *Int J Radiat Oncol Biol Phys* 2008;70(4):1002–10. [PubMed: 18313524]
27. Cao Y. Development of Image Software Tools for Radiation Therapy Assessment. *Medical Physics* 2005;32:2136.
28. Tofts PS, Brix G, Buckley DL, Evelhoch JL, Henderson E, Knopp MV, Larsson HB, Lee TY, Mayr NA, Parker GJ, Port RE, Taylor J, Weisskoff RM. Estimating kinetic parameters from dynamic contrast-enhanced T(1)- weighted MRI of a diffusible tracer: standardized quantities and symbols. *J Magn Reson Imaging* 1999;10(3):223–32. [PubMed: 10508281]
29. Tombaugh TN. Trail Making Test A and B: normative data stratified by age and education. *Arch Clin Neuropsychol* 2004;19(2):203–14. [PubMed: 15010086]
30. Benedict RH, Zgaljardic DJ. Practice effects during repeated administrations of memory tests with and without alternate forms. *J Clin Exp Neuropsychol* 1998;20(3):339–52. [PubMed: 9845161]

31. Benedict RHB, Schretlen D, Groninger L, Brandt J. Hopkins Verbal Learning Test -- Revised: normative data and analysis of inter-form and test-retest reliability. *Clin Neuropsychologist* 1998;12:43–55.
32. Lezak, M.; D. *Neuropsychological Assessment*. Oxford University Press; New York: 1995.
33. Spreen, O.; Strauss, E. *A compredium of neuropsychological tests*. Oxford University Press; New York: 1998.
34. Merchant TE, Kiehna EN, Li C, Xiong X, Mulhern RK. Radiation dosimetry predicts IQ after conformal radiation therapy in pediatric patients with localized ependymoma. *Int J Radiat Oncol Biol Phys* 2005;63(5):1546–54. [PubMed: 16115736]
35. Cao Y, Tsien CI, Shen Z, Tatro DS, Ten Haken R, Kessler ML, Chenevert TL, Lawrence TS. Use of magnetic resonance imaging to assess blood-brain/blood-glioma barrier opening during conformal radiotherapy. *J Clin Oncol* 2005;23(18):4127–36. [PubMed: 15961760]
36. Yuan H, Gaber MW, Boyd K, Wilson CM, Kiani MF, Merchant TE. Effects of fractionated radiation on the brain vasculature in a murine model: blood-brain barrier permeability, astrocyte proliferation, and ultrastructural changes. *Int J Radiat Oncol Biol Phys* 2006;66(3):860–6. [PubMed: 17011458]
37. Hodges H, Katzung N, Sowinski P, Hopewell JW, Wilkinson JH, Bywaters T, Rezvani M. Late behavioural and neuropathological effects of local brain irradiation in the rat. *Behav Brain Res* 1998;91(1–2):99–114. [PubMed: 9578444]
38. Cao Y, Pan C, Balter JM, Platt JF, Francis IR, Knol JA, Normolle D, Ben-Josef E, Ten Haken RK, Lawrence TS. Liver function after irradiation based on computed tomographic portal vein perfusion imaging. *Int J Radiat Oncol Biol Phys* 2008;70(1):154–60. [PubMed: 17855011]

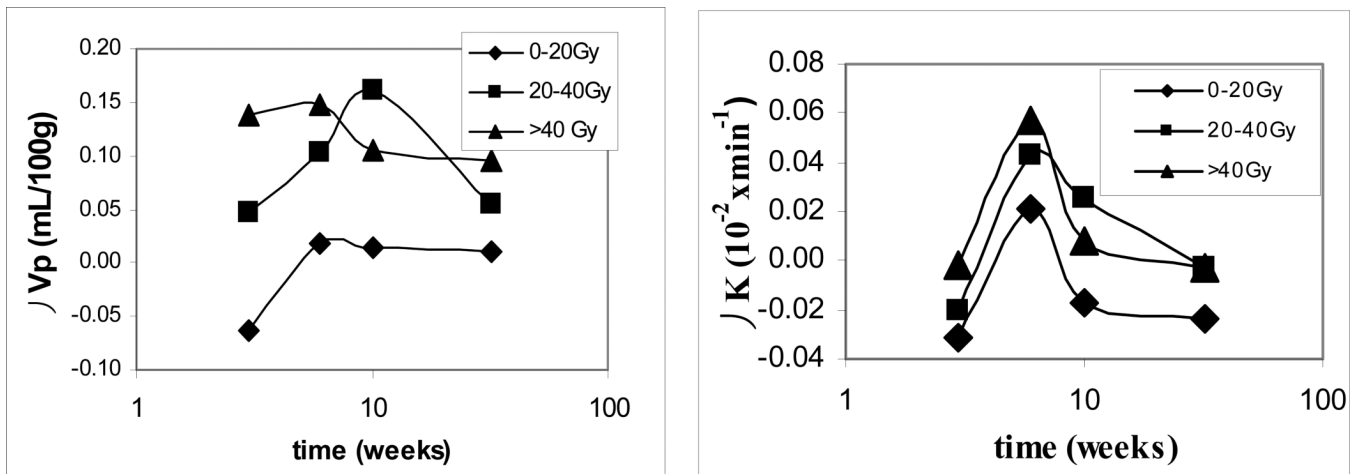


Figure 1.

The differences in the vascular volumes (V_p) and blood-brain barrier permeability (K^{trans}) in three dose intervals at three observation times compared to the baseline values. In the high dose region (> 40 Gy), the vascular volumes increased significantly at week 6 during the course of RT and then started decreasing after the completion of RT; while in the intermediate dose interval (20–40 Gy), the vessel volume increased slowly, reached the similar maximum value 1 month after the completion of RT, and then started decreasing. The changes in the blood-brain barrier permeability were significant in the high and intermediate dose regions at week 6 during the course of RT. 10 weeks: 1 month after the completion of RT; and 32 weeks: 6 months after the completion of RT.

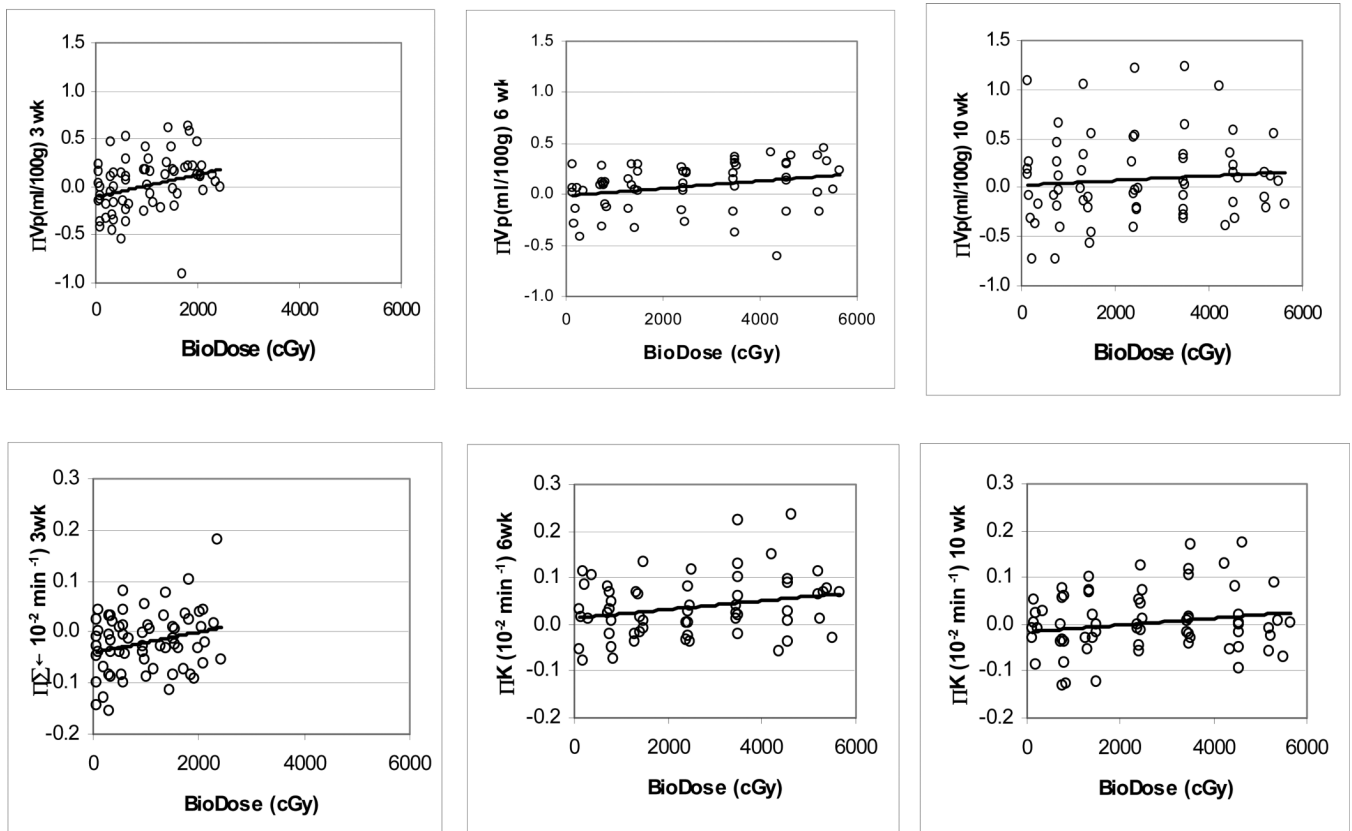


Figure 2.

Scatter plots of the changes in the vascular volumes (V_p , top) and blood-brain permeability (K^{trans} , bottom) versus doses received at the time of MRI studies. Left panels: week 3 during RT; Middle panels: week 6 during RT; Right panels: 1 month after the completion of RT (10 weeks from the start of RT). Solid lines represent linear regression lines.

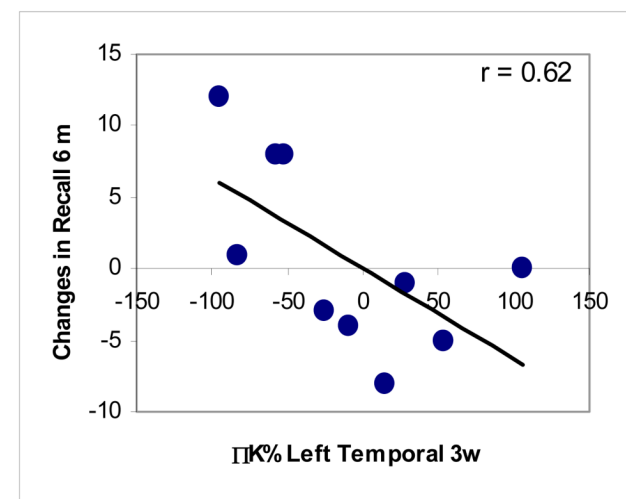
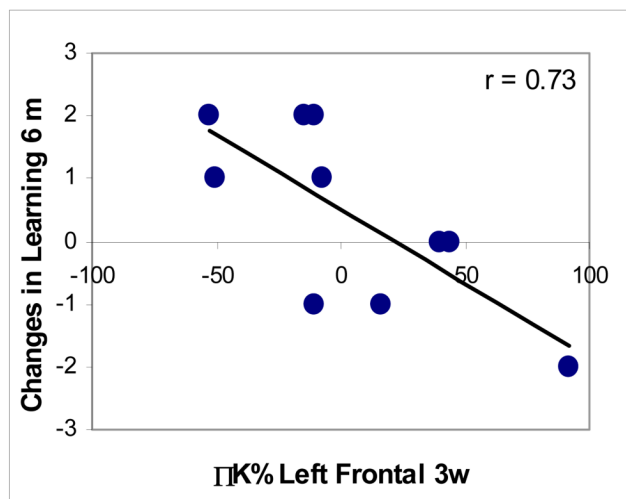
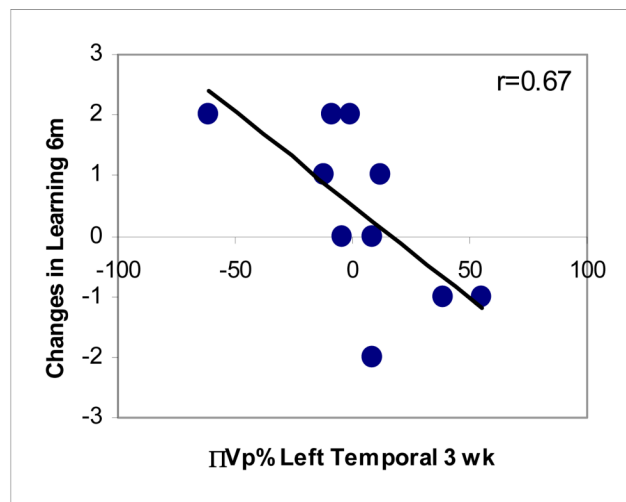
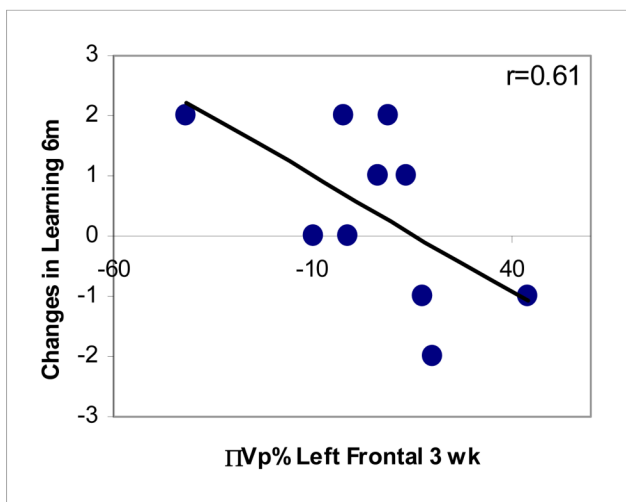


Figure 3. The correlations between the changes in learning scores 6 months after RT and the changes in Vp of left frontal (left top) and temporal (right top) lobes at week 3 during RT, between the changes in learning scores 6 months after RT and the changes in K^{trans} of left frontal lobes at week3 during RT (left bottom), and between the changes in total recall scores 6 months after RT and the changes in K^{trans} of left temporal lobes at week 3 during RT (right bottom).

Table 1

Patient demographics, primary diagnosis, and radiation dose

Patient	Age(year)/Sex	Diagnosis	Location	Prescribed Dose (Gy)	Fx Size (Gy)/No Fx
1	33/M	Grade II Gemistocytic Astrocytoma	R Temporal	59.4	1.8/33
2	64/M	Pituitary macroadenoma	Suprasellar	50.4	1.8/28
3	55/M	Sphenoid Wing Meningioma	L Medial Sphenoid	54.0	1.8/30
4	29/M	Cranopharyngioma	Suprasellar	55.8	1.8/31
5	25/F	Low Grade Glioma	L Frontal	54.0	1.8/30
6	71/M	Null Cell Pituitary Adenoma	Suprasellar	50.4	1.8/28
7	36/M	WHO III anaplastic supratentorial ependyoma	L Frontal	59.4	1.8/33
8	55/M	Grade II Astrocytoma	Bifrontal	54.0	1.8/30
9	39/M	Grade II Mixed Oligoastrocytoma	R Frontotemporal	59.4	1.8/33
10	44/M	Pituitary macroadenoma	Suprasellar	50.4	1.8/28

Fx: fraction; L: left; R: right.

Table 2

Linear mixed models

time	3 weeks		6 weeks		10 weeks		32 weeks	
	β_t	P	β_t	P	β_t	P	β_t	P
V_p								
Model 1	1.1×10^{-2}	0.0001	4.8×10^{-3}	0.0002	3.6×10^{-3}	0.001		n.s.
Model 2	3.5×10^{-5}	0.0001	1.3×10^{-5}	0.0001	1.3×10^{-5}	0.0001	7.3×10^{-6}	0.007
K^{trans}								
Model 1	2.0×10^{-5}	0.001	7.8×10^{-6}	0.03	6.1×10^{-6}	0.001	4.5×10^{-6}	0.03

Model 1 includes dose effects, while model 2 includes dose-volume effects. Units of β_t : (ml/100g) per Gy for Model 1 of V_p , (ml/100g) per Gy per cc for Model 2 of V_p , and per min per Gy for Model 1 of K^{trans} . Weeks were counted from the start of RT. 10 weeks: 1 month after the completion of RT; 32 weeks: 6 months after the completion of RT.

Table 3

MMSE and HVLТ Scores

patients	MMSE Pre-RT, 1m, 6m	HVLТ Total Recall Pre-RT, 1m, 6m	HVLТ Learning Pre-RT, 1m, 6m	Delayed Recall Pre-RT, 1m, 6m
1	30, 30, 30	26, 25, 34	3, 4, 2	9, 10, 11
2	27, 27, 28	17, * 23, 29	4, 5, 6	9, 10, 9
3	28, 26, 29	5, * 14, 13	1, + 2, 1	0, * 2, 1
4	30, 30, 30	33, 26, 25	3, 6, 3	12, 12, 12
5	29, 30, 30	28, 29, 28	5, 6, 3	12, 12, 12
6	27, 26, 28	16, * 17, 15	3, 0, 4	5, 5, 6
7	28, 30, 30	29, 24, 30	3, 4, 4	8, 7, 11
8	29, 27, 27	19, * 26, 14	1, + 3, 3	7, * 9, 5
9	30, 30, 29	26, 21, 23	1, + 2, 3	8, 6, 9
10	30, 29, 29	23, + 22, 19	4, 3, 3	7, * 7, 7

1m: 1 month post RT; 6m: 6 months post RT; Maximum score of MMSE = 30; Maximum score for total recall = 36; Maximum score delayed recall = 12.

* score is < 1.5 SD below the mean of the age-matched normative data

+ score is equal to 1.5 SD below the mean of the age-matched normative data (borderline value)